Article

Catalytic enantioselective nucleophilic desymmetrization of phosphonate esters

Michele Formica[1], Tatiana Rogova [1], Heyao Shi[1], Naoto Sahara[1,2], Branislav Ferko[1], Alistair J. M. Farley [1], Kirsten E. Christensen [1], Fernanda Duarte [1], Ken Yamazaki [3] ✉ & Darren J. Dixon [1] ✉

Molecules that contain a stereogenic phosphorus atom are crucial to medicine, agrochemistry and catalysis. While methods are available for the selective construction of various chiral organophosphorus compounds, catalytic enantioselective approaches for their synthesis are far less common. Given the vastness of possible substituent combinations around a phosphorus atom, protocols for their preparation should also be divergent, providing facile access not only to one but to many classes of phosphorus compounds. Here we introduce a catalytic and enantioselective strategy for the preparation of an enantioenriched phosphorus(V) centre that can be diversified enantiospecifically to a wide range of biologically relevant phosphorus(V) compounds. The process, which involves an enantioselective nucleophilic substitution catalysed by a superbasic bifunctional iminophosphorane catalyst, can accommodate a wide range of carbon substituents at phosphorus. The resulting stable, yet versatile, synthetic intermediates can be combined with a multitude of medicinally relevant O-, N- and S-based nucleophiles.

Compounds containing one or more stereogenic phosphorus atoms in the P(V) oxidation state are important to chemistry, biology and medicine[1]. These include marketed antiviral drugs such as Tenofovir alafenamide and Remdesivir[2], an effective treatment for Ebola that has also recently been approved for use against SARS-CoV-2. Existing approaches for the stereoselective synthesis of P-stereogenic centres, while elegant, remain mostly diastereoselective, with catalytic enantioselective approaches being limited in application. Accordingly, divergent, broad-scope, catalytic strategies for the efficient stereoselective synthesis of diverse stereogenic P(V)-containing compounds remain essential[3,4].

To this end, we describe an enantioselective two-stage strategy, exploiting a catalytic and highly enantioselective[5–7] desymmetrization[8] of phosphonate esters. Pivoting on a stereocontrolled, sequential nucleophilic substitution of enantiotopic leaving groups from readily accessible prochiral P(V) precursors, a bifunctional iminophosphorane (BIMP)[9–11] superbase catalyst was found to be essential in delivering reactive desymmetrized intermediates capable

of downstream enantiospecific substitution. This uniquely modular, catalytic platform allows broad-scope, stereoselective access to a diverse library of chiral P(V) compounds including those with O, N and S linkages.

Over the past few years, substantial progress has been made in improving the synthesis of P(V) chiral compounds. In 2017, Merck reported a diastereoselective dynamic kinetic asymmetric transformation (DYKAT) to synthesize MK-3682, a lead ProTide (ref. 12) antiviral compound as well as other analogues[13]. The process was reliant on a chiral C2 symmetric nucleophilic organocatalyst, which provided the desired prodrug with exquisite diastereocontrol from racemic P(V) starting material.

Recently, the Baran group reported a highly versatile chiral P(V) reagent: PSI (ψ), derived from limonene, for the diastereoselective synthesis of phosphorothioate oligonucleotides and of cyclic dinucleotides (CDNs)[14,15]. Building upon previous chiral auxiliary approaches[16–21], this work was also expanded towards the synthesis of P-chiral phosphines, as well as methylphosphonate oligonucleotides (MPOs)[22].

[1]Chemistry Research Laboratory, Department of Chemistry, University of Oxford, Oxford, UK. [2]Graduate School of Engineering, Nagoya University, Nagoya, Japan. [3]Division of Applied Chemistry, Okayama University, Okayama, Japan. ✉e-mail: k-yamazaki@okayama-u.ac.jp; darren.dixon@chem.ox.ac.uk
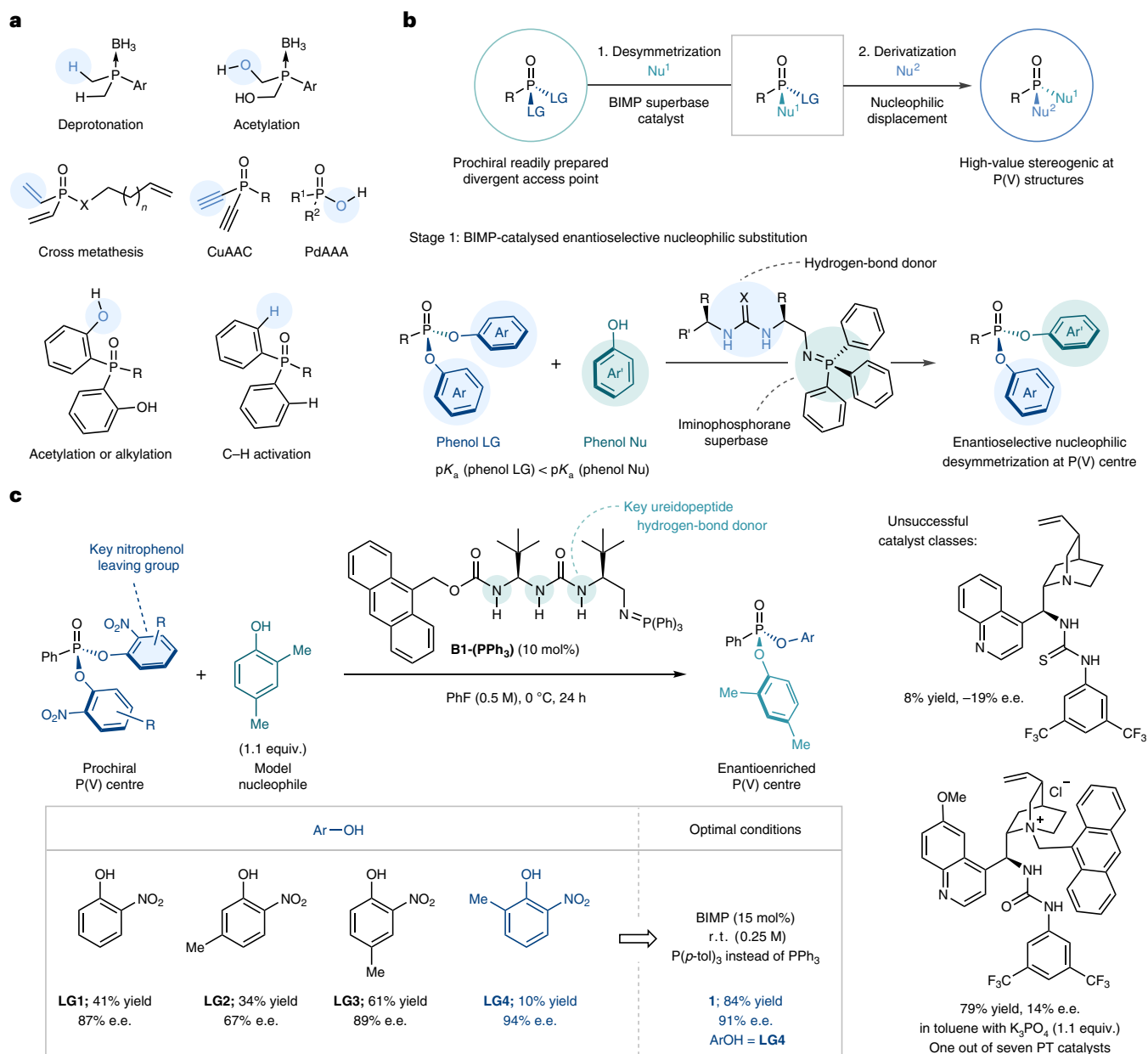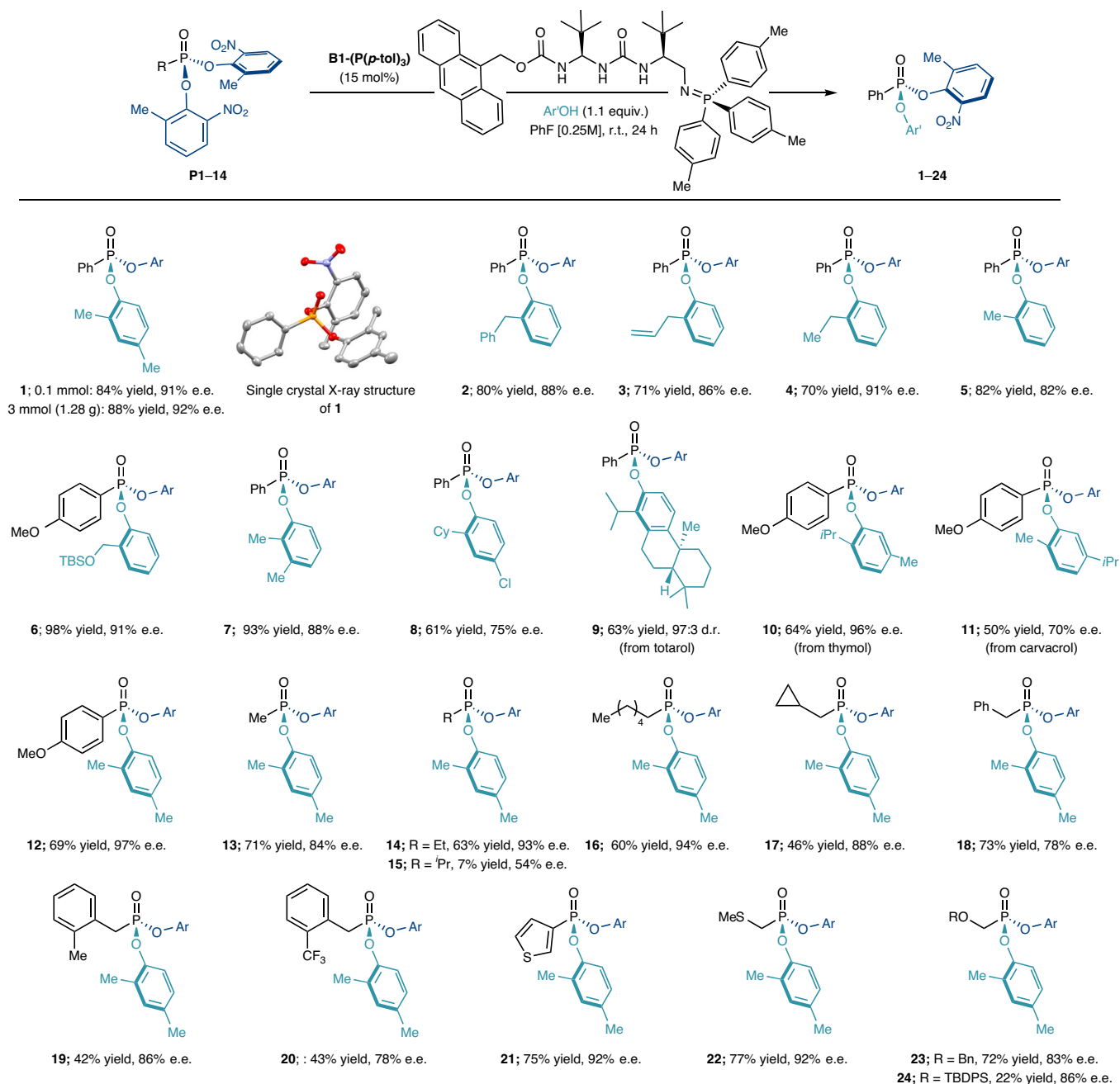
Fig. 1 | Previous work, reaction design and optimisation. a, State-of-the-art in catalytic enantioselective desymmetrization of P(V) compounds. **b**, A two-phase strategy for the construction of diverse enantioenriched P(V) compounds consisting of a bifunctional iminophosphorane-catalysed enantioselective nucleophilic substitution and downstream enantiospecific modification of the resulting enantioenriched intermediate. **c**, Effect of the nature of the leaving group on reaction efficiency and selectivity (left) with representative unsuccessful catalyst classes (right). CuAAC, copper-catalysed azide–alkyne cycloaddition; PdAAA, palladium-catalysed asymmetric allylic alkylation; LG, leaving group; Nu, nucleophile; r. t., room temperature; PT, phase transfer.

While these elegant processes towards P-chiral compounds are effective, they remain diastereoselective, where the absolute stereo-chemical configuration at the phosphorus centre is controlled either through a matched combination of catalyst and a carefully tailored starting material or by employing a stoichiometric chiral leaving group. Notwithstanding sophisticated, contemporary enantioselective aryla-tion[23,24] and allylation[25] protocols of secondary phosphine oxides (lim-ited to all carbon substituents on phosphorus), a few notable reports have also been seen where a P-stereogenic centre is generated indirectly through the functionalization of enantiotopic P-bound groups. How-ever, this approach inherently limits the scope and application of these protocols (Fig. 1a)[26–36]. Despite these impressive advances, to date, no catalytic enantioselective desymmetrization protocols have been established with reactivity occurring directly at the phosphorus atom[37]

(following the disclosure of this work as a preprint and while this paper was under revision, an elegant and complementary catalytic enantiose-lective nucleophilic desymmetrization of phosphoryl dichlorides was published by the Jacobsen group[38]).

We envisioned a two-stage desymmetrization–derivatization strategy by which enantiotopic phenolic leaving groups on a prochiral phosphonate ester are enantiodiscriminated by a suitable nucleophile under the control of a chiral Brønsted base catalyst[39], generating a new P–O bond. The resulting enantioenriched intermediate would retain suitable reactivity for sequential substitution of the remaining leaving group. With appropriate stereocontrol, this uniquely modular approach would overcome the key restrictions of previously developed protocols. Given the tunability and high basicity of our bifunctional iminophosphorane catalysts[9–11], we expected that they would provide

Table 1 | Scope of the desymmetrization reaction with respect to the phenol nucleophile and electrophilic P(V) substrate

1; 0.1 mmol: 84% yield, 91% e.e.
3 mmol (1.28 g): 88% yield, 92% e.e.

Single crystal X-ray structure of **1**

2; 80% yield, 88% e.e.

3; 71% yield, 86% e.e.

4; 70% yield, 91% e.e.

5; 82% yield, 82% e.e.

6; 98% yield, 91% e.e.

7; 93% yield, 88% e.e.

8; 61% yield, 75% e.e.

9; 63% yield, 97:3 d.r. (from totarol)

10; 64% yield, 96% e.e. (from thymol)

11; 50% yield, 70% e.e. (from carvacrol)

12; 69% yield, 97% e.e.

13; 71% yield, 84% e.e.

14; R = Et, 63% yield, 93% e.e.
15; R = ^{i}Pr, 7% yield, 54% e.e.

16; 60% yield, 94% e.e.

17; 46% yield, 88% e.e.

18; 73% yield, 78% e.e.

19; 42% yield, 86% e.e.

20; : 43% yield, 78% e.e.

21; 75% yield, 92% e.e.

22; 77% yield, 92% e.e.

23; R = Bn, 72% yield, 83% e.e.
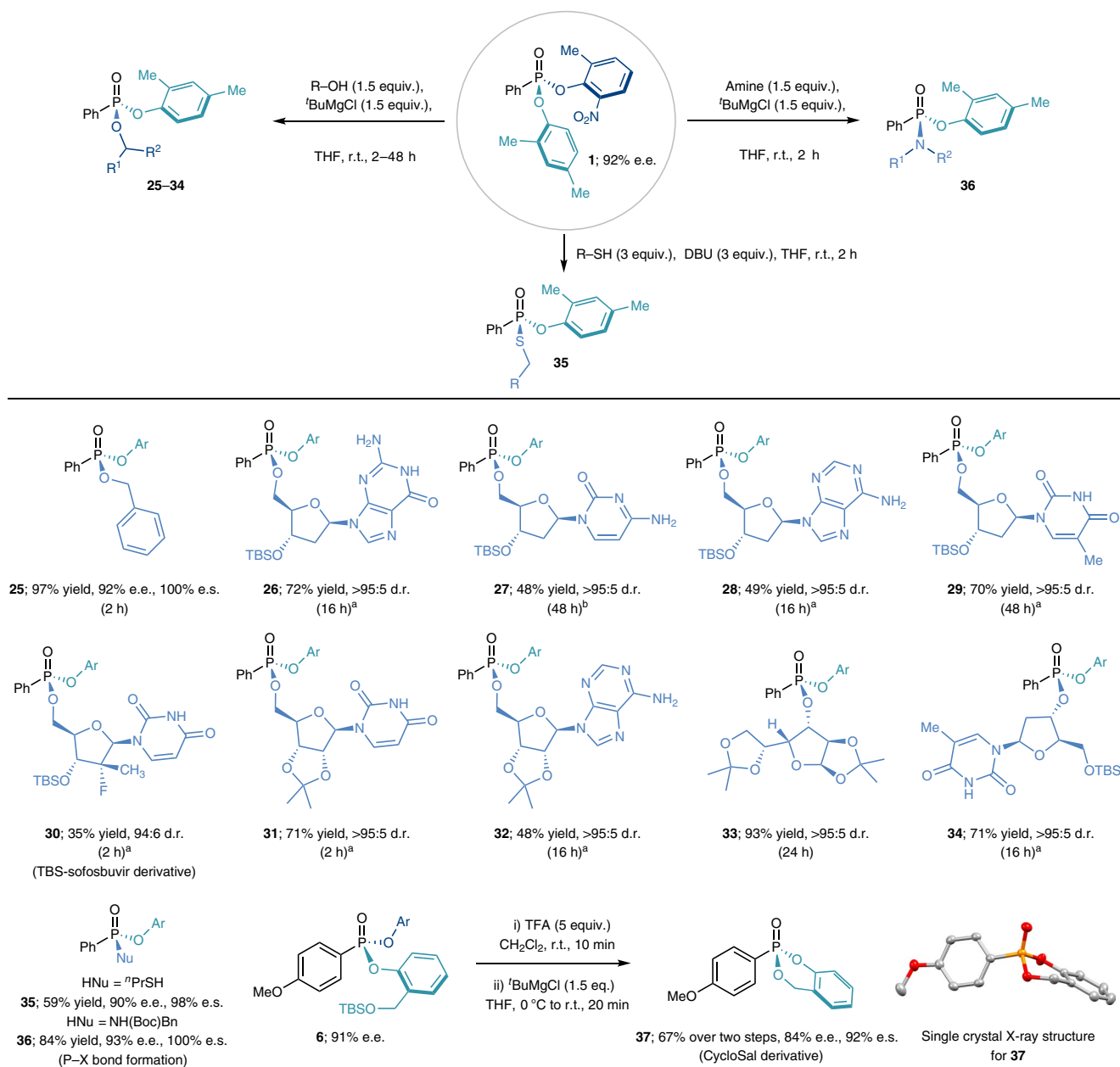**24**; R = TBDPS, 22% yield, 86% e.e.

Bn, benzyl; Cy, cyclohexyl; TBS, *tert*-butyldimethylsilyl; TBDPS, *tert*-butyldiphenylsilyl; r. t., room temperature.

sufficient pronucleophile/substrate activation and could be suitably adapted to obtain high levels of enantiopurity in the products (Fig. 1b).

Results and discussion

To explore the proposed reaction design, we began our investigations by identifying an appropriate model system containing a phosphonyl dichloride mimic, utilizing 2,4-dimethylphenol as the nucleophile and a BIMP superbase catalyst. The leaving group had to possess key characteristics based on the dichotomy between leaving group ability/basicity and stability of the P(V) precursor to allow for reactivity and catalyst turnover. After a comprehensive investigation of potential leaving groups, *para*-nitrophenol was identified to possess good reactivity as well as crucially permitting catalyst turnover[40] (Supplementary Scheme 1).

Following this key breakthrough, a survey of nitrophenol isomers resulted in *ortho*-nitrophenol (**LG1**) being identified as optimal for enantioselectivity. The development of a new BIMP catalyst bearing a ureidopeptide hydrogen-bond donor motif (**B1**), inspired by the work of Palomo[41–43], and tuning of the reaction conditions led to a first lead result of 41% yield and 87% e.e. (Fig. 1c). To augment catalyst turnover, the pK_a of the leaving group was carefully adjusted by introducing a methyl-group at different positions around the aromatic ring of the nitrophenol (**LG2**–**LG4**). While the installation of a methyl group at the 4-position (**LG3**) gave the best yield (61%), a methyl group at the 6-position (**LG4**) gave optimal enantioselectivity (94% e.e.) albeit with a drop in reactivity. By conducting the reaction at room temperature and fine-tuning the basicity of the catalyst (exchanging PPh₃ with P(*p*-tol)₃

Table 2 | Derivatization of the desymmetrized enantioenriched P(V) products

R–OH (1.5 equiv.), ^{t}BuMgCl (1.5 equiv.), THF, r.t., 2–48 h — **25–34**

Amine (1.5 equiv.), ^{t}BuMgCl (1.5 equiv.), THF, r.t., 2 h — **36**

R–SH (3 equiv.), DBU (3 equiv.), THF, r.t., 2 h — **35**

1; 92% e.e.

25; 97% yield, 92% e.e., 100% e.s. (2 h)

26; 72% yield, >95:5 d.r. (16 h)[a]

27; 48% yield, >95:5 d.r. (48 h)[b]

28; 49% yield, >95:5 d.r. (16 h)[a]

29; 70% yield, >95:5 d.r. (48 h)[a]

30; 35% yield, 94:6 d.r. (2 h)[a] (TBS-sofosbuvir derivative)

31; 71% yield, >95:5 d.r. (2 h)[a]

32; 48% yield, >95:5 d.r. (16 h)[a]

33; 93% yield, >95:5 d.r. (24 h)

34; 71% yield, >95:5 d.r. (16 h)[a]

HNu = ^{n}PrSH
35; 59% yield, 90% e.e., 98% e.s.
HNu = NH(Boc)Bn
36; 84% yield, 93% e.e., 100% e.s.
(P–X bond formation)

6; 91% e.e.

i) TFA (5 equiv.) CH$_2$Cl$_2$, r.t., 10 min
ii) ^{t}BuMgCl (1.5 eq.) THF, 0 °C to r.t., 20 min

37; 67% over two steps, 84% e.e., 92% e.s. (CycloSal derivative)

Single crystal X-ray structure for **37**

P–O bond formation, P–S and P–N bond formation and synthesis of a cycloSal prodrug derivative. [a] ^{t}BuMgCl (3 equiv.) was used. [b] ^{t}BuMgCl (4 equiv.) was used. DBU, 1,8-diazabicyclo(5.4.0) undec-7-ene; TBS, *tert*-butyldimethylsilyl; TFA, trifluoroacetic acid; Bn, benzyl; Boc, *tert*-butyloxycarbonyl; r.t., room temperature.

for the generation of the iminophosphorane), the yield of product **1** was increased to 84% and its e.e. was found to be 91%. For comparison, it is worthy of note that both Cinchona-derived bifunctional organocatalysts and phase-transfer catalysis were ineffective in providing the desired product in high yield and enantioselectivity (Supplementary Schemes 2 and 3).

With the optimized conditions in hand, we proceeded to explore the scope of this enantioselective nucleophilic desymmetrization (Table 1). We were pleased to find that a variety of phenols possessing *ortho*-substituents (**2**–**6**) were well tolerated and high yields and enantioselectivities were maintained. Compound **6** (98% yield, 91% e.e.) is of particular interest as a precursor to cycloSal-type prodrugs[44]. 2,3-Disubstituted phenols were also found to be effective nucleophiles (**7**). The introduction of electron-withdrawing groups (**8**) was also possible, despite a slight reduction in enantioselectivity. Bulky,

naturally occurring phenols totarol and thymol were also competent nucleophiles for delivering the desymmetrized P(V) products (**9**, **10**) in good yield and high enantioselectivity. Importantly, when totarol was reacted with **P1**, catalysed by achiral base BEMP (2-*tert*-butylimino-2-d iethylamino-1,3-dimethylperhydro-1,3,2-diazaphosphorine), no diastereoselectivity was observed, demonstrating that the stereoselective reaction was under complete catalyst control. Using carvacrol as a nucleophile (**11**) resulted in diminished enantioselectivity. Nucleophiles bearing no *ortho*-substituent were found to afford the corresponding products in good yields but poor enantioselectivity, confirming that the *ortho*-substituent was a key discriminating feature in the transition structures governing the stereoselectivity of the reaction. Additionally, heterocyclic phenols or alkyl alcohols were found to be unreactive under the optimized conditions (Supplementary Scheme 8). The reaction was also successful on a gram scale (3 mmol)
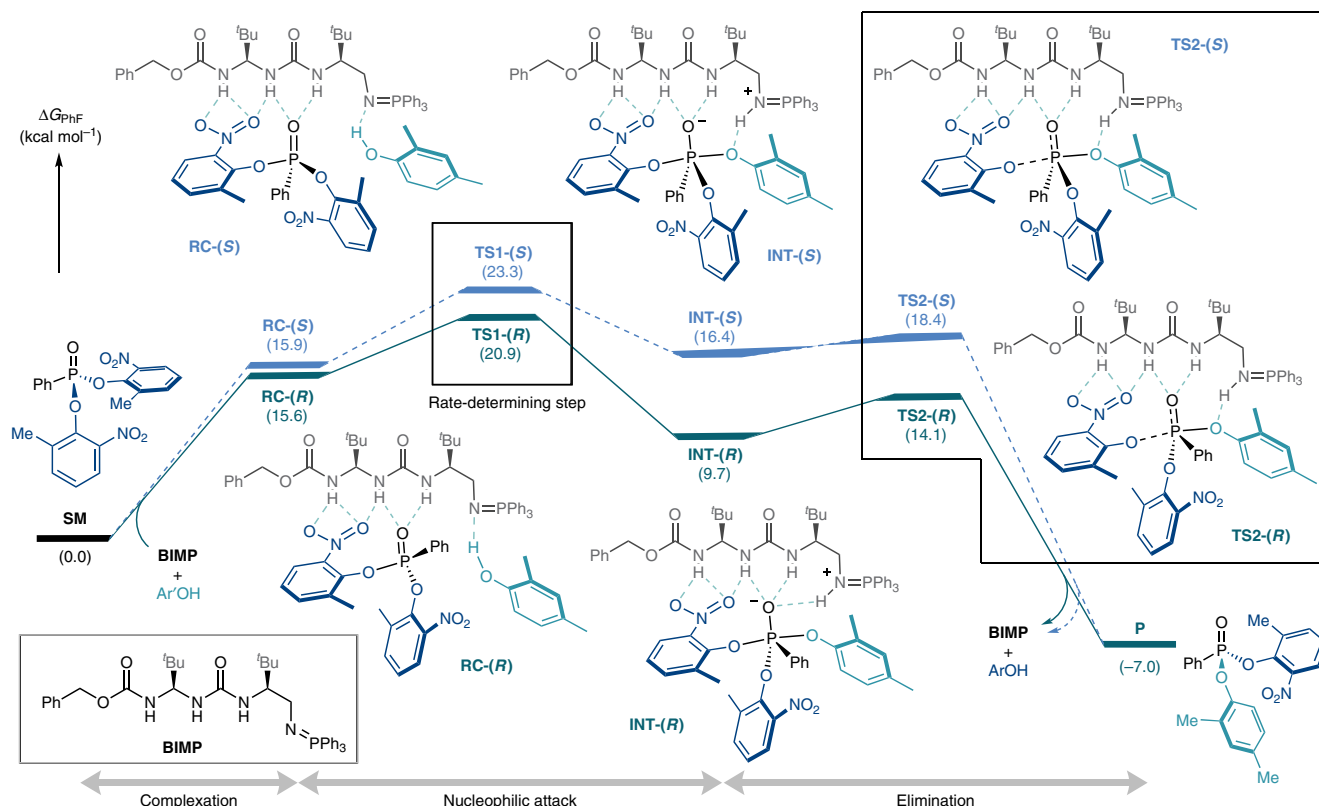
Fig. 2 | DFT study. Potential energy surface [ΔG (kcal mol^{-1})] for the enantioselective nucleophilic desymmetrization of the P(V) compound **P1** with 2-methyl-6-nitrophenol using the model BIMP catalyst **B12-P(Ph)$_3$** computed at the SMD(fluorobenzene)/M06-2X/def2TZVP//SMD(fluorobenzene)/ M06-2X/def2SVP level of theory. The reaction was found to proceed in three stages: complexation, nucleophilic attack and elimination from a metastable pentacoordinate intermediate. The rate- (and enantio-) determining step was found to be nucleophilic addition of the phenol to **P1** with the TS leading to the (R)-product (**TS1-(R)**) being more favourable than that leading to the (S)-product (**TS1-(S)**) by 2.4 kcal mol^{-1}. Gibbs free energies (kcal mol^{-1}) are reported in parenthesis. ArOH, 2-methyl-6-nitrophenol; Ar′OH, 2,4-dimethylphenol; SM, starting material.

with no loss in yield or enantioselectivity. Desymmetrized product **1** was recrystallized to >99.9% e.e. and the absolute stereochemical configuration was assigned as (R) by single crystal X-ray diffraction analysis (see Supplementary Data 1–2). Having probed the scope of the nucleophilic partner, we proceeded to vary the P-linked carbon substituent on the phosphonate ester electrophile. Such changes were broadly tolerated with aryl (**12**), methyl (**13**), higher alkyl (**14**, **16**) and β-branched (**17**) substituents maintaining high reaction efficiency and enantioselectivities. Substrates containing α-branched substituents (**15**) were less reactive, resulting in low yield of product and diminished enantioselectivity, most probably due to the increased steric hindrance around the P atom. Benzyl substituents (**18**–**20**) were also tolerated, albeit with a slight decrease in selectivity. Finally, we were pleased to find that thiophene (**21**)- and (thio)ether (**22**, **23**)-substituted prochiral phosphorus electrophiles were also competent substrates for our methodology. Once again, increasing the steric demand around the P atom by installing a *tert*-butyldiphenylsilyl (TBDPS) silyl ether (**24**) resulted in diminished reactivity. However, in this case, good enantioselectivity was maintained.

Having established the scope of the desymmetrization for both the nucleophilic and electrophilic components, we proceeded to assess the crucial second stage of the strategy: the enantiospecific nucleophilic substitution of the remaining nitrophenol leaving group (Table 2). After a preliminary investigation into the applicability of existing protocols, we found that Lewis acid activation of the P(V) species, pioneered by Merck[45], was highly efficient in promoting the second nucleophilic displacement. Indeed, treating compound **1** with 1.5 equiv. each of *t*BuMgCl and benzyl alcohol in THF at room temperature smoothly afforded mixed phosphonate ester **25** in almost

quantitative yield and 100% enantiospecificity (e.s.). Encouraged by this success, we proceeded to use more complex and biologically relevant alcohols as nucleophiles. All four DNA nucleosides (**26**–**29**), hepatitis C treatment sofosbuvir (**30**) as well as acetal-protected uridine (**31**) and adenosine (**32**) were successfully phosphorylated at the 5′-OH with moderate to good yields and >95:5 d.r. Acetal-protected D-glucose (**33**) and deoxythymidine (**34**) were both phosphorylated at the more hindered secondary 3′-OH in excellent yields and diastereoselectivity. Having established reactivity with alcohol nucleophiles we proceeded to investigate the stereocontrolled formation of alternative P-heteroatom linkages. However, when using *n*-propanethiol as the nucleophile, no desired product was obtained when using *t*BuMgCl to promote the reaction. The main by-product observed was (2-methyl-6-nitrophenyl)(propyl)thioether, obtained via an S$_N$Ar mechanism. This obstacle was overcome by switching the promoter to 3 equiv. of DBU (1,8-diazabicyclo(5.4.0)undec-7-ene), which gave the desired thiophosphonate ester **35** in 59% yield and 98% e.s.. We then turned our attention to N-centred nucleophiles and were thrilled to find that when using *N*-Boc benzylamine (Boc, *tert*-butyloxycarbonyl) as the nucleophile we could obtain phosphonamidite ester **36** in 84% yield and 100% e.s. Finally, *tert*-butyldimethylsilyl (TBS)-protected phosphonate ester **6** was deprotected with trifluoroacetic acid (TFA) and cyclized with *t*BuMgCl to give cycloSal derivative **37** in 67% yield and 92% e.s. over two steps. Upon recrystallization to enantiopurity and single crystal X-ray diffraction analysis (see Supplementary Data 1–2), the absolute configuration of **37** was determined to be (R), showing inversion of configuration[21,46–48] with respect to the starting material. To confirm the importance of controlling stereochemical configuration at all substitution steps, acetal-protected uridine and D-glucose were also
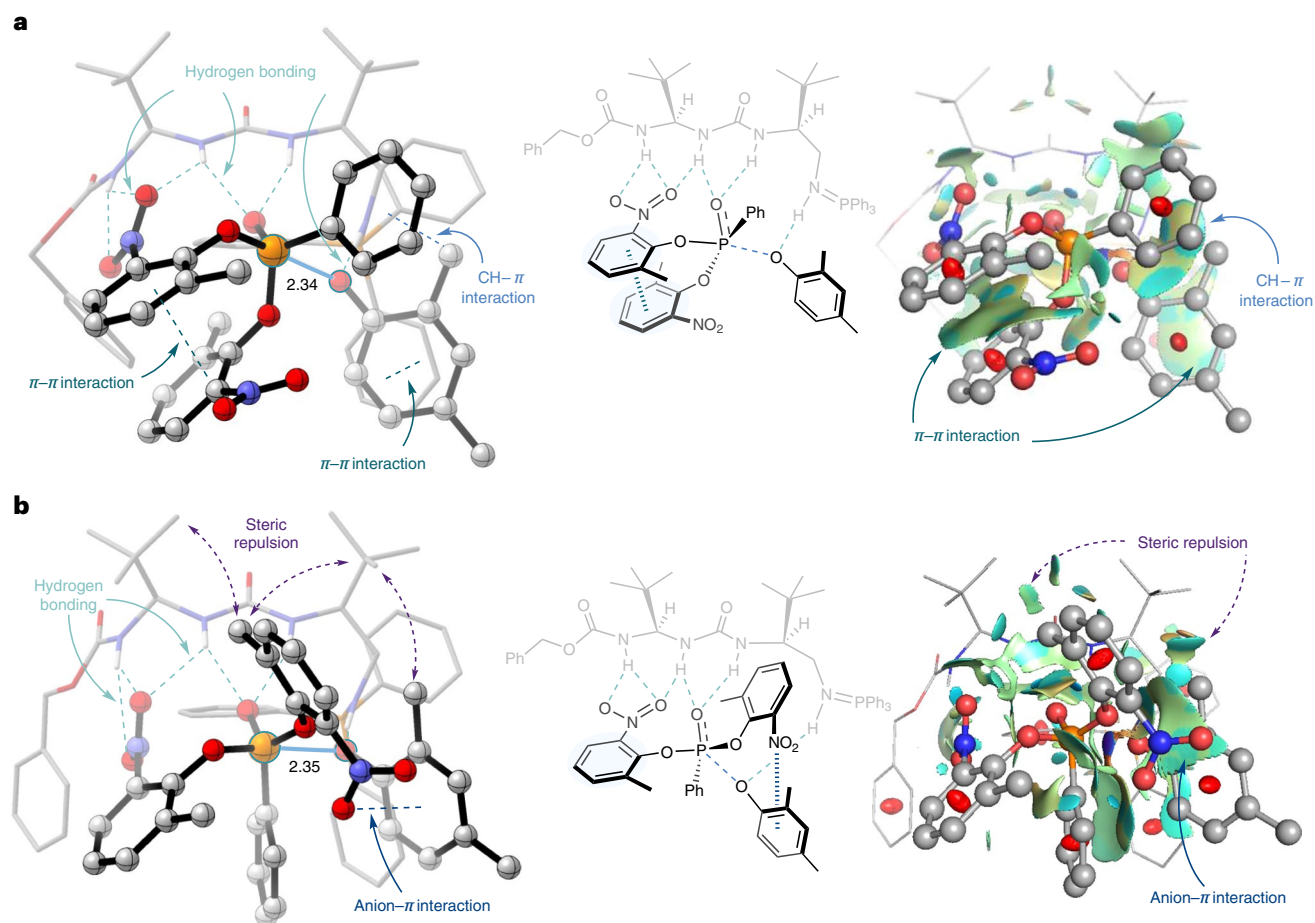
Fig. 3 | Rate-determining nucleophilic attack TS structures and the visualization of the NCI surfaces. a, Three-dimensional structures of **TS1-(R)** for the formation of the (R)-product. **b**, Three-dimensional structures of **TS1-(S)** for the formation of the (S)-product. Bond lengths of the TS geometries are given in Å. NCI surfaces are represented as the coloured regions in the figure.

Multiple stabilising inter- and intra-molecular NCIs such as hydrogen bonding, π–π and CH–π interactions are observed in the favoured TS **TS1-(R)**, while the destabilizing steric repulsion between the substrate, nucleophile and catalyst exists in the unfavoured TS **TS1-(S)**.

reacted with racemic **1**. Both compounds **31** and **33** were obtained as a 1:1 mixture of diastereoisomers, thus highlighting the importance of deploying enantioenriched **1** in the second nucleophilic substitution to obtain a single diastereomeric product (see NMR data for compounds **31** and **33** in the Supplementary Information for details).

To further probe the mechanism and establish the origins of enantioselectivity, a computational density functional theory (DFT) study was undertaken[47–50]. The catalysed reaction was modelled with **B12-P(Ph)₃** containing a benzyloxycarbonyl (Cbz) carbamate and a triphenylphosphine-derived iminophosphorane moiety (Fig. 2). The computed potential energy surfaces indicated that the initial nucleophilic attack for the formation of the pentacoordinate intermediate is the rate- and enantio-determining step. Pleasingly, the favoured transition state (TS) **TS1-(R)** leads to the desymmetrized product with experimentally confirmed absolute stereochemical configuration by single crystal X-ray diffraction studies ($\Delta\Delta G^{\ddagger} = 2.4$ kcal mol^{-1}), and the predicted enantioselectivity of 97% e.e. is in good agreement with the experimental selectivity of 92% e.e. Once the pentacoordinate intermediate **INT-(R)** is obtained, the carbamate-assisted facile elimination of the nitrophenol group occurs through **TS2-(R)** to furnish the desymmetrized product.

To obtain further insight into the origin of enantioselectivity with the optimized BIMP catalyst, the TS structures for the initial nucleophilic attack were analysed (Fig. 3). The favoured TS conformation in **TS1-(R)** engages in several stabilizing non-covalent interactions (NCIs)

such as hydrogen bonding, π–π and CH–π interactions (Fig. 3a). The notable characteristic feature is that the two nitrophenol aromatic rings are tightly bound by a π–π interaction, which, in the absence of significant steric repulsions, stabilises the TS. On the other hand, the disfavoured TS **TS1-(S)** does not display such an interaction. Instead, steric repulsion between the substrate, nucleophile and catalyst can be observed that could contribute to destabilizing the TS (Fig. 3b). A qualitative analysis of the NCI surfaces provided further evidence of the existence of the above-mentioned interactions for the origin of enantioselectivity[51]. Furthermore, the specific roles of substituents in the optimized catalyst and substrates were examined by calculating the key nucleophilic attack TS structures with different catalyst backbones, which were later verified experimentally (Supplementary Fig. 1). Specifically, the *t*-Bu groups on the catalyst and the *ortho*-methyl group of the nucleophile contribute to destabilizing the disfavoured TS structure due to steric repulsion. On the other hand, the *ortho*-nitro group of the leaving group is required for the substrate to bind to the catalyst tightly via hydrogen-bond interactions. The insights gained from both experiments and computation demonstrate that key NCIs arising from the tunable nature of the catalyst and leaving group are vital for the observed catalytic and enantioselective efficiency.

In conclusion, a two-stage strategy for the synthesis of stereogenic P(V) compounds through an unprecedented enantioselective nucleophilic desymmetrization and subsequent enantiospecific derivatization, was developed. A BIMP catalyst bearing a ureidopeptide

hydrogen-bond donor moiety provided a unique chiral environment and sufficient pronucleophile/substrate activation to allow the desymmetrization to proceed with excellent yield and enantioselectivity. Through judicious choice of leaving group, facile downstream diversification of the desymmetrized P(V) ester with a multitude of medicinally relevant nucleophiles with very high enantiospecificity was allowed. This study represents a clear strategic departure from previously established catalytic methods that rely on substrate engineering and do not easily allow for facile downstream modification to medicinally attractive molecules. Finally, DFT studies were carried out to elucidate an energetically plausible reaction pathway for the two enantiomeric products and to uncover the main attractive NCIs responsible for the high levels of enantioselectivity observed for the major enantiomer. This conceptually novel, two-stage desymmetrization/derivatization approach has enabled modular catalytic enantioselective access to stereogenic P(V) compounds by a strategy that we hope will unlock new opportunities and inspire further developments in the field.

Online content

Any methods, additional references, Nature Portfolio reporting summaries, source data, extended data, supplementary information, acknowledgements, peer review information; details of author contributions and competing interests; and statements of data and code availability are available at https://doi.org/10.1038/s41557-023-01165-6.

References

1. Rodriguez, J. B. & Gallo-Rodriguez, C. The role of the phosphorus atom in drug design. *ChemMedChem* **14**, 190–216 (2018).
2. Siegel, D. et al. Therapeutic efficacy of the small molecule GS-5734 against Ebola virus in rhesus monkeys. *Nature* **531**, 381–385 (2016).
3. Dutartre, M., Bayardon, J. & Jugé, S. Applications and stereoselective syntheses of P-chirogenic phosphorus compounds. *Chem. Soc. Rev.* **45**, 5771–5794 (2016).
4. Zhou, J. et al. Recent advances in catalytic asymmetric synthesis of *P*-chiral phosphine oxides. *Acta Chim. Sin.* **78**, 193–216 (2020).
5. Liu, S. et al. First catalytic enantioselective synthesis of P-stereogenic phosphoramides via kinetic resolution promoted by a chiral bicyclic imidazole nucleophilic catalyst. *Tetrahedron: Asymmetry* **23**, 329–332 (2012).
6. Tamura, T. & Ryukoku, E. Asymmetric synthesis of organic phosphorus compounds. Japan patent JP 2003128688 A (2003).
7. Wang, L. et al. Organocatalytic enantioselective synthesis of P-stereogenic chiral oxazaphospholidines. *Eur. J. Org. Chem.* **2016**, 2024–2028 (2016).
8. Borissov, A. et al. Organocatalytic enantioselective desymmetrisation. *Chem. Soc. Rev.* **45**, 5474–5540 (2016).
9. Núñez, M. G., Farley, A. J. M. & Dixon, D. J. Bifunctional iminophosphorane organocatalysts for enantioselective synthesis: application to the ketimine nitro-Mannich reaction. *J. Am. Chem. Soc.* **135**, 16348–16351 (2013).
10. Farley, A. J. M., Sandford, C. & Dixon, D. J. Bifunctional iminophosphorane catalyzed enantioselective sulfa-Michael addition to unactivated α-substituted acrylate esters. *J. Am. Chem. Soc.* **137**, 15992–15995 (2015).
11. Formica, M., Rozsar, D., Su, G., Farley, A. J. M. & Dixon, D. J. Bifunctional iminophosphorane superbase catalysis: applications in organic synthesis. *Acc. Chem. Res.* **53**, 2235–2247 (2020).
12. Mehellou, Y., Rattan, H. S. & Balzarini, J. The ProTide prodrug technology: from the concept to the clinic. *J. Med. Chem.* **61**, 2211–2226 (2018).
13. DiRocco, D. A. et al. A multifunctional catalyst that stereoselectively assembles prodrugs. *Science* **356**, 426–430 (2017).
14. Knouse, K. W. et al. Unlocking P(V): Reagents for chiral phosphorothioate synthesis. *Science* **361**, 1234–1238 (2018).
15. Huang, Y. et al. P(V)-platform for oligonucleotide synthesis. *Science* **373**, 1265–1270 (2021).
16. Juge, S., Stephan, M., Laffitte, J. A. & Genet, J. P. Efficient asymmetric synthesis of optically pure tertiary mono and diphosphine ligands. *Tetrahedron Lett.* **31**, 6357–6360 (1990).
17. Juge, S. & Genet, J. P. Asymmetric synthesis of phosphinates, phosphine oxides and phosphines by Michaelis Arbuzov rearrangement of chiral oxazaphospholidine. *Tetrahedron Lett.* **30**, 2783–2786 (1989).
18. Corey, E. J., Chen, Z. & Tanoury, G. J. A new and highly enantioselective synthetic route to P-chiral phosphines and diphosphines. *J. Am. Chem. Soc.* **115**, 11000–11001 (1993).
19. Han, Z. S. et al. Efficient asymmetric synthesis of *P*-chiral phosphine oxides via properly designed and activated benzoxazaphosphinine-2-oxide agents. *J. Am. Chem. Soc.* **135**, 2474–2477 (2013).
20. Kuwabara, K., Maekawa, Y., Minoura, M., Maruyama, T. & Murai, T. Chemoselective and stereoselective alcoholysis of binaphthyl phosphonothioates: straightforward access to both stereoisomers of biologically relevant *P*-stereogenic phosphonothioates. *J. Org. Chem.* **85**, 14446–14455 (2020).
21. Mondal, A., Thiel, N. O., Dorel, R. & Feringa, B. L. P-chirogenic phosphorus compounds by stereoselective Pd-catalysed arylation of phosphoramidites. *Nat. Catal.* **5**, 10–19 (2021).
22. Xu, D. et al. Enantiodivergent formation of C–P bonds: synthesis of P-chiral phosphines and methylphosphonate oligonucleotides. *J. Am. Chem. Soc.* **142**, 5785–5792 (2020).
23. Beaud, R., Phipps, R. J. & Gaunt, M. J. Enantioselective Cu-catalyzed arylation of secondary phosphine oxides with diaryliodonium salts toward the synthesis of P-chiral phosphines. *J. Am. Chem. Soc.* **138**, 13183–13186 (2016).
24. Dai, Q., Li, W., Li, Z. & Zhang, J. P-chiral phosphines enabled by palladium/Xiao-Phos-catalyzed asymmetric P–C cross-coupling of secondary phosphine oxides and aryl bromides. *J. Am. Chem. Soc.* **141**, 20556–20564 (2019).
25. Liu, X., Zhang, Y.-Q., Han, X., Sun, S. & Zhang, Q. Ni-catalyzed asymmetric allylation of secondary phosphine oxides. *J. Am. Chem. Soc.* **141**, 16584–16589 (2019).
26. Diesel, J. & Cramer, N. Generation of heteroatom stereocenters by enantioselective C–H functionalization. *ACS Catal.* **9**, 9164–9177 (2019).
27. Genov, G. R., Douthwaite, J. L., Lahdenperä, A. S. K., Gibson, D. C. & Phipps, R. J. Enantioselective remote C–H activation directed by a chiral cation. *Science* **367**, 1246–1251 (2020).
28. Huang, Q.-H. et al. Access to *P*-stereogenic compounds *via* desymmetrizing enantioselective bromination. *Chem. Sci.* **68**, 42–61 (2021).
29. Wiktelius, D., Johansson, M. J., Luthman, K. & Kann, N. A biocatalytic route to P-chirogenic compounds by lipase-catalyzed desymmetrization of a prochiral phosphine–borane. *Org. Lett.* **7**, 4991–4994 (2005).
30. Toda, Y., Pink, M. & Johnston, J. N. Brønsted acid catalyzed phosphoramidic acid additions to alkenes: diastereo- and enantioselective halogenative cyclizations for the synthesis of *C*- and *P*-chiral phosphoramidates. *J. Am. Chem. Soc.* **136**, 14734–14737 (2014).
31. Harvey, J. S. et al. Enantioselective synthesis of P-stereogenic phosphinates and phosphine oxides by molybdenum-catalyzed asymmetric ring-closing metathesis. *Angew. Chem. Int. Ed.* **48**, 762–766 (2009).

32. Trost, B. M., Spohr, S. M., Rolka, A. B. & Kalnmals, C. A. Desymmetrization of phosphinic acids via Pd-catalyzed asymmetric allylic alkylation: rapid access to P-chiral phosphinates. *J. Am. Chem. Soc.* **141**, 14098–14103 (2019).

33. Zhu, R.-Y., Chen, L., Hu, X.-S., Zhou, F. & Zhou, J. Enantioselective synthesis of *P*-chiral tertiary phosphine oxides with an ethynyl group *via* Cu(I)-catalyzed azide–alkyne cycloaddition. *Chem. Sci.* **11**, 97–106 (2020).

34. Yang, G., Li, Y., Li, X. & Cheng, J.-P. Access to P-chiral phosphine oxides by enantioselective allylic alkylation of bisphenols. *Chem. Sci.* **10**, 4322–4327 (2019).

35. Zheng, Y., Guo, L. & Zi, W. Enantioselective and regioselective hydroetherification of alkynes by gold-catalyzed desymmetrization of prochiral phenols with P-stereogenic centers. *Org. Lett.* **20**, 7039–7043 (2018).

36. Zhang, Y. et al. Asymmetric synthesis of *P*-stereogenic compounds via thulium(III)-catalyzed desymmetrization of dialkynylphosphine oxides. *ACS Catal.* **9**, 4834–4840 (2019).

37. Lemouzy, S., Giordano, L., Hérault, D. & Buono, G. Introducing chirality at phosphorus atoms: an update on the recent synthetic strategies for the preparation of optically pure P-stereogenic molecules. *Eur. J. Org. Chem.* **2020**, 3351–3366 (2020).

38. Forbes, K. C. & Jacobsen, E. N. Enantioselective hydrogen-bond-donor catalysis to access diverse stereogenic-at-P(V) compounds. *Science* **376**, 1230–1236 (2022).

39. Wang, Y.-H. et al. Activating pronucleophiles with high pK_a values: chiral organo-superbases. *Angew. Chem. Int. Ed.* **59**, 8004–8014 (2020).

40. Greenhalgh, M. D., Qu, S., Slawin, A. M. Z. & Smith, A. D. Multiple roles of aryloxide leaving groups in enantioselective annulations employing α,β-unsaturated acyl ammonium catalysis. *Chem. Sci.* **9**, 4909–4918 (2018).

41. Diosdado, S. et al. Catalytic enantioselective synthesis of tertiary thiols from 5*H*-thiazol-4-ones and nitroolefins: bifunctional ureidopeptide-based Brønsted base catalysis. *Angew. Chem. Int. Ed.* **52**, 11846–11851 (2013).

42. Diosdado, S., Lõpez, R. & Palomo, C. Ureidopeptide-based Brønsted bases: design, synthesis and application to the catalytic enantioselective synthesis of β-amino nitriles from (arylsulfonyl) acetonitriles. *Chem. Eur. J.* **20**, 6526–6531 (2014).

43. Vera, S. et al. Synthesis of β-hydroxy α-amino acids through Brønsted base-catalyzed *syn*-selective direct aldol reaction of Schiff bases of glycine o-nitroanilide. *J. Org. Chem.* **86**, 7757–7772 (2021).

44. Meier, C. *cyclo*Sal phosphates as chemical trojan horses for intracellular nucleotide and glycosylmonophosphate delivery—chemistry meets biology. *Eur. J. Org. Chem.* **2006**, 1081–1102 (2006).

45. Simmons, B., Liu, Z., Klapars, A., Bellomo, A. & Silverman, S. M. Mechanism-based solution to the ProTide synthesis problem: selective access to sofosbuvir, Acelarin, and INX-08189. *Org. Lett.* **19**, 2218–2221 (2017).

46. Kolodiazhnyi, O. I. in *Asymmetric Synthesis in Organophosphorus Chemistry: Synthetic Methods, Catalysis, and Applications* (ed. Kolodiazhnyi, O. I.) 35–99 (Wiley-VCH Verlag GmbH & Co. KGaA, 2016).

47. Van Bochove, M. A., Swart, M. & Bickelhaupt, F. M. Nucleophilic substitution at phosphorus ($S_N2@P$): disappearance and reappearance of reaction barriers. *J. Am. Chem. Soc.* **128**, 10738–10744 (2006).

48. Van Bochove, M. A., Swart, M. & Bickelhaupt, F. M. Stepwise walden inversion in nucleophilic substitution at phosphorus. *Phys. Chem. Chem, Phys.* **11**, 259–267 (2009).

49. Kolodiazhnyi, O. I. & Kolodiazhna, A. Nucleophilic substitution at phosphorus: stereochemistry and mechanisms. *Tetrahedron: Asymmetry* **28**, 1651–1674 (2017).

50. Kirby, A. J. & Nome, F. Fundamentals of phosphate transfer. *Acc. Chem. Res.* **48**, 1806–1814 (2015).

51. Boto, R. A. et al. NCIPLOT4: fast, robust, and quantitative analysis of noncovalent interactions. *J. Chem. Theory Comput.* **16**, 4150–4158 (2020).

Methods

To the corresponding organoazide (0.015 mmol) and tris-*para*-tolylphosphine (0.015 mmol) under an argon atmosphere was added THF (0.40 ml). Then the reaction mixture was stirred for 24 h at room temperature. The formation of the organocatalysts was monitored by thin-layer chromatography. Upon completion volatiles were removed under a stream of N_2, yielding the expected iminiphosphorane (**B1-(P(*p*-tol)$_3$**)) that was used without further purification.

To the corresponding phosphonate (0.10 mmol) and BIMP organocatalyst (0.015 mmol) under an argon atmosphere was added PhF (0.40 ml) and phenol (0.11 mmol, 1.1 equiv.). The reaction mixture was stirred at room temperature for 24 h. Then it was loaded directly onto silica gel and purified by flash column chromatography to afford pure desymmetrized phosphonate ester.

Reporting summary

Further information on research design is available in the Nature Portfolio Reporting Summary linked to this article.

Data availability

Crystallographic data are available free of charge from the Cambridge Crystallographic Data Centre under references CCDC 2097043 (**1**) and CCDC 2097044 (**37**). Additional optimization data, full synthetic methods and characterization data are available in the Supplementary Information.

Author contributions

M.F. and D.J.D. conceived the project. M.F., T.R., H.S., N.S. and B.F. conducted all experimental work and analysed the data. A.J.M.F. designed and first synthesized the ureidopeptide BIMP catalyst. K.Y. conducted the computational work based on preliminary studies carried out by T.R. and F.D. Single-crystal X-ray diffraction experiments were conducted by K.E.C. The manuscript was written by M.F., K.Y. and D.J.D. with contributions and proof-reading from all authors. D.J.D. directed the project.

Competing interests

The authors declare no competing interests.

Additional information

Supplementary information The online version contains supplementary material available at https://doi.org/10.1038/s41557-023-01165-6.

Correspondence and requests for materials should be addressed to Ken Yamazaki or Darren J. Dixon.

Peer review information *Nature Chemistry* thanks Zhengxu Han, Xin Li and the other, anonymous, reviewer(s) for their contribution to the peer review of this work.

Reprints and permissions information is available at www.nature.com/reprints.

Corresponding author(s): Ken Yamazaki, Darren J. Dixon

Last updated by author(s): 2022/08/19

Reporting Summary

Nature Portfolio wishes to improve the reproducibility of the work that we publish. This form provides structure for consistency and transparency in reporting. For further information on Nature Portfolio policies, see our Editorial Policies and the Editorial Policy Checklist.

Statistics

For all statistical analyses, confirm that the following items are present in the figure legend, table legend, main text, or Methods section.

n/a	Confirmed	
☒	☐	The exact sample size (n) for each experimental group/condition, given as a discrete number and unit of measurement
☒	☐	A statement on whether measurements were taken from distinct samples or whether the same sample was measured repeatedly
☒	☐	The statistical test(s) used AND whether they are one- or two-sided *Only common tests should be described solely by name; describe more complex techniques in the Methods section.*
☒	☐	A description of all covariates tested
☒	☐	A description of any assumptions or corrections, such as tests of normality and adjustment for multiple comparisons
☒	☐	A full description of the statistical parameters including central tendency (e.g. means) or other basic estimates (e.g. regression coefficient) AND variation (e.g. standard deviation) or associated estimates of uncertainty (e.g. confidence intervals)
☒	☐	For null hypothesis testing, the test statistic (e.g. F, t, r) with confidence intervals, effect sizes, degrees of freedom and P value noted *Give P values as exact values whenever suitable.*
☒	☐	For Bayesian analysis, information on the choice of priors and Markov chain Monte Carlo settings
☒	☐	For hierarchical and complex designs, identification of the appropriate level for tests and full reporting of outcomes
☒	☐	Estimates of effect sizes (e.g. Cohen's d, Pearson's r), indicating how they were calculated

Our web collection on statistics for biologists contains articles on many of the points above.

Software and code

Policy information about availability of computer code

Data collection	N/A
Data analysis	N/A

For manuscripts utilizing custom algorithms or software that are central to the research but not yet described in published literature, software must be made available to editors and reviewers. We strongly encourage code deposition in a community repository (e.g. GitHub). See the Nature Portfolio guidelines for submitting code & software for further information.

Data

Policy information about availability of data

All manuscripts must include a data availability statement. This statement should provide the following information, where applicable:
- Accession codes, unique identifiers, or web links for publicly available datasets
- A description of any restrictions on data availability
- For clinical datasets or third party data, please ensure that the statement adheres to our policy

Provide your data availability statement here.

Human research participants

Policy information about [studies involving human research participants and Sex and Gender in Research.](#)

Reporting on sex and gender	N/A
Population characteristics	N/A
Recruitment	N/A
Ethics oversight	N/A

Note that full information on the approval of the study protocol must also be provided in the manuscript.

Field-specific reporting

Please select the one below that is the best fit for your research. If you are not sure, read the appropriate sections before making your selection.

☒ Life sciences   ☐ Behavioural & social sciences   ☐ Ecological, evolutionary & environmental sciences

For a reference copy of the document with all sections, see [nature.com/documents/nr-reporting-summary-flat.pdf](#)

Life sciences study design

All studies must disclose on these points even when the disclosure is negative.

Sample size	N/A
Data exclusions	N/A
Replication	N/A
Randomization	N/A
Blinding	N/A

Reporting for specific materials, systems and methods

We require information from authors about some types of materials, experimental systems and methods used in many studies. Here, indicate whether each material, system or method listed is relevant to your study. If you are not sure if a list item applies to your research, read the appropriate section before selecting a response.

Materials & experimental systems

n/a	Involved in the study
☒ ☐	Antibodies
☒ ☐	Eukaryotic cell lines
☒ ☐	Palaeontology and archaeology
☒ ☐	Animals and other organisms
☒ ☐	Clinical data
☒ ☐	Dual use research of concern

Methods

n/a	Involved in the study
☒ ☐	ChIP-seq
☒ ☐	Flow cytometry
☒ ☐	MRI-based neuroimaging